

Spectra and Light Curve Analysis of Nova V475 Scuti

G. E. MORGAN,¹ F. A. RINGWALD,^{1,2} C. BUIL,³ AND M. GARRETT⁴

Received 2005 May 4; accepted 2005 May 25; published 2005 August 1

ABSTRACT. This paper collects together early IAU Circular observations, plots the light curve, and presents our own spectra of V475 Scuti (Nova Sct 2003). We describe the early spectral evolution of this nova during the 7 weeks after its discovery. The principal spectra show this nova to be a common Fe II type (R. E. Williams et al.). The nova displayed dominant Balmer lines and numerous Fe II multiplets (42, 48, 49, 55, and 74), with strong, well-distributed P Cygni profiles that disappeared near the end of our observations. Spectral evolution produced low-ionization forbidden lines consistent with an auroral phase (R. E. Williams et al.). V475 Sct was a fast nova, with $t_2 = 22$ days and with a type Ba light curve (H. W. Duerbeck) from the American Association of Variable Star Observers. The H α velocity widths showed a twofold increase, together with an unusual *broadening* of the line, during our observations. The lack of structure within the high-resolution H α profiles suggests that the nova is exhibiting an isotropic expansion as an optically thick wind, which may result in material falling back onto the white dwarf. We encourage further monitoring.

1. INTRODUCTION

Nova eruptions are among the most powerful explosions observed in our Galaxy. They are often bright enough to be studied with small telescopes. Time-resolved spectroscopy taken during the nova eruption allows for the physical study of the eruption, the nuclear reactions that power it, and for the measurement of the expansion of the fireball thrown off from the underlying star system. This study is part of an ongoing program (Morgan et al. 2003) to explore changes in the spectra and light curves of novae over time, in order to test the classification system of Williams et al. (1991, 1994).

Reports of Nova V475 Sct first appeared in IAU Circulars 8190 (Nakano et al. 2003), IAU Circulars 8191 (Boeche et al. 2003), IAU Circulars 8199 (Siviero et al. 2003), and IAU Circulars 8200 (Samus et al. 2003). The information in the circulars is summarized as follows. Discovery was made by H. Nishimura on 2003 August 28.6 UT (JD 2,452,880.1) at a visual magnitude of 8.5 (Nakano et al. 2003). Spectra quickly confirmed this to be a classical nova (Boeche et al. 2003), with H α emission showing a width (FWHM) of 300 km s⁻¹ at August 31.093 UT and 700 km s⁻¹ at August 31.55 UT, and complex P Cygni profiles on September 6.83 (Siviero et al. 2003). Precise astrometry for this nova is summarized in Tables 1 and 2.

In § 2, we describe our observations. In § 3, we present new spectra, both low and high resolution, and compile a light curve from reported observations. In § 4, we discuss the features of this system, particularly an observed broadening of the Balmer and other emission lines.

2. OBSERVATIONS

We collected 10 low-resolution spectra and 6 high-resolution spectra. Six of the low-resolution spectra were collected by C. Buil at Castanet Tolosan Observatory in France. These spectra were taken with a slitless Littrow spectrograph with a 600 line mm⁻¹ grating in the Meris setup (described in detail by Buil 2003⁵) using a Kodak KAF-402E CCD detector at a 0.287 nm pixel⁻¹ dispersion through a Nikon 135 mm f/2.8 collimating lens and a Nikon 50 mm f/1.4 objective lens. This setup was used with a 128 mm Takahashi refractor. The remaining four low-resolution spectra were collected at the Campus Observatory at California State University, Fresno, using a Santa Barbara Instrument Group (SBIG) self-guiding spectrograph (SGS) with a 100 μ m slit, a 150 line mm⁻¹ grating, and an SBIG ST-7XE Kodak KAF-0401E CCD, at a dispersion of 0.432 nm pixel⁻¹. These spectra were collected through a 406 mm Meade LX-200 Schmidt-Cassegrain telescope.

All six of the high-resolution spectra were collected by C. Buil at Castanet Tolosan. The first two high-resolution H α spectra were collected in the LHIRES setup (C. Buil 2003; see footnote 5) with the slitless Littrow spectrograph, using a 1200 line mm⁻¹ grating. The nova image was spread over a Kodak KAF-1602E CCD with a 0.023 nm pixel⁻¹ dispersion through a 300 mm collimating and objective lens, used with a 128 mm

¹ Central Valley Astronomers, Incorporated, P.O. Box 3063, Pinedale, CA 93650.

² Department of Physics, California State University, Fresno, 2345 East San Ramon Avenue, MS MH37, Fresno, CA 93740-8031; ringwald@csufresno.edu.

³ Castanet Tolosan Observatory, 6 Place Clemence Isaure, 31320 Castanet Tolosan, France; christian.buil@wanadoo.fr.

⁴ Department of Chemistry, California State University, Fresno, 2555 East San Ramon Avenue, MS SB70, Fresno, CA 93740-0700.

⁵ See <http://www.astrosurf.com/buil>.

TABLE 1
ASTROMETRIC FIGURES (EQUINOX 2000.0)

Author	Location	R.A.	Decl.	Reference
S. Nakano & H. Sato	Nat. Astron. Obs. Japan (NAJO)	18 49 38	−09 33 45	IAU Circ. 8190
T. Nakamura & S. Wakuda		18 49 37.62	−09 33 50.3	IAU Circ. 8190
H. Yamaoka	Kyushu Univ.	18 49 37.600	−09 33 50.85	IAU Circ. 8199
A. Henden	US Naval Obs.	18 49 37.602	−09 33 50.76	IAU Circ. 8199

NOTE.—Units of right ascension are hours, minutes, and seconds, and units of declination are degrees, arcminutes, and arcseconds.

Takahashi refractor. The remaining four of the six high-resolution spectra of the H α line were taken in the HIRES setup, using Buil's configuration, but with a 180 mm Nikon f/2.8 collimating and objective lens that gave a 0.038 nm pixel^{−1} dispersion with a 212 mm f/3.5 Takahashi Newtonian telescope.

Data reduction for all setups included dark and bias frame subtractions, flat-field divisions, and night-sky subtractions. Wavelength calibrations were made with a mercury standard lamp and were referenced to the H₂O-vapor telluric absorption lines near the H α emission line. No flux standards were taken, but the instrumental response was removed by normalizing the spectra. Table 3 summarizes the observational details of the spectra collected in this study.

3. DATA ANALYSIS

3.1. Light Curve Data

Light curve data reported and validated by the American Association of Variable Star Observers (AAVSO) are shown in Figure 1. This shows that maximum brightness occurred on JD 2,452,884.3 \pm 0.5 at $V_{\max} = 8.0 \pm 0.2$. The light curve is not smooth. The median brightness held relatively constant near magnitude 9.0 \pm 0.8 for about 3 weeks and then shifted to magnitude 10.0 \pm 0.8 for 4 weeks. Minor irregular variations of about 1.5 mag peak-to-peak were observed, with a rapid decrease in brightness after 7 weeks to a point that made any additional data collection impractical for our optical setups.

The light curve is consistent with a type Ba light curve, as described by Duerbeck (1981), including a decline with standstills or other minor irregular fluctuations. Values for t_2 and t_3 can be measured easily for smooth, concave type-A light curves. Type Ba light curves with minor irregular variations make accurate t_2 and t_3 measurements more difficult. Our best estimates for $t_2 = 22$ days and $t_3 = 52$ days for V475 Sct, making it a fast novan as defined by Duerbeck (1981). Warner (1989) noted

a correlation of t_2 and t_3 values to be $t_3 \sim 2.75 t_2^{0.88}$. This relationship holds only loosely, since the light curve of V475 Sct exhibits a convex shape rather than the more common concave shape for fast novae.

3.2. Low-Resolution Spectra

We wanted to see whether this nova's spectral evolution followed the classification sequence of Williams et al. (1991,

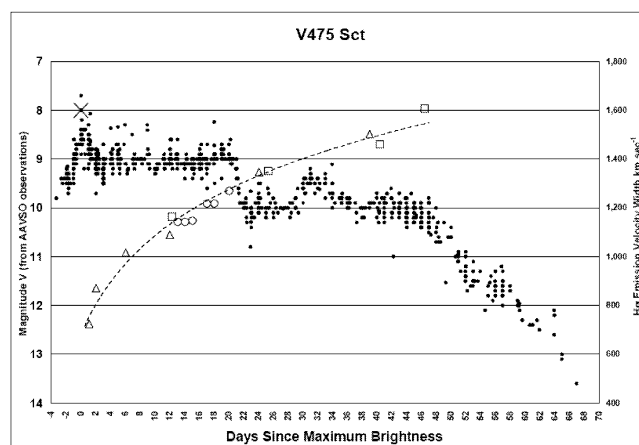


FIG. 1.—Plot of AAVSO light curve data for V475 Sct. Maximum brightness is marked with a cross (X) and occurred on JD 2,452,884.3 \pm 0.5 days at $V_{\max} = 8.0 \pm 0.2$. The nova maintained brightness (values on the left axis) at about magnitude 9 for 3 weeks, then magnitude 10 for 4 weeks, with variations of about 1.5 mag peak-to-peak prior to a rapid decrease in brightness. With a t_2 of 22 days, V475 Sct was a fast nova with a Duerbeck (1981) type Ba light curve. The dates spectra were collected are marked by the open triangles for C. Buil's low-resolution data, open circles for Buil's high-resolution data, and open squares for Fresno low-resolution data. The H α emission velocity widths (values on the right axis) increased twofold during our observations.

TABLE 2
PROBABLE PROGENITOR STAR (EQUINOX 2000.0)

Catalog	Number	B	R	R.A.	Decl.	Reference
GSC 2	S00220349902	17.2	...	18 49 37.70	−09 33 54.1	IAU Circ. 8190
USNO-B1.0	0804-00484139	17.47	15.87	18 49 37.70	−09 33 54.1	IAU Circ. 8190
USNO-A2.0	0750-148 33804	17.2	16.4	18 49 37.684	−09 33 53.76	IAU Circ. 8190

NOTE.—Units of right ascension are hours, minutes, and seconds, and units of declination are degrees, arcminutes, and arcseconds.

TABLE 3
OBSERVATION LOG

Data Number	HJD (UT) - 2,452,000	Magnitude (V)	Days $T_{\max} +$	Observer and Instrument	Resolution (nm)	Range λ	Dispersion (nm pixel ⁻¹)	Exposures (N × min)	Air Mass
Low-Resolution Data									
1	885.415	9.0	1	Buil Tak FS-128 Meris	0.7	Vis.	0.287	12 × 2	1.96
2	886.333	9.0	2	Buil Tak FS-128 Meris	0.7	Vis., Red	0.287	16 × 2	1.67
3	890.355	9.0	6	Buil Tak FS-128 Meris	0.7	Vis.	0.287	11 × 2	1.71
4	896.315	9.0	12	Buil Tak FS-128 Meris	0.7	Vis., Red	0.287	20 × 2	1.67
5	896.594	9.0	12	Fresno LX-200 406 SGS	3	Vis., Red	0.432	3 × 10	1.52
6	908.346	10.0	24	Buil Tak FS-128 Meris	0.7	Vis.	0.287	15 × 2	1.92
7	909.593	10.0	25	Fresno LX-200 406 SGS	3	Vis., Red	0.432	4 × 10	1.45
8	923.293	10.0	39	Buil Tak FS-128 Meris	0.7	Vis.	0.287	24 × 2	1.85
9	924.692	10.0	40	Fresno LX-200 406 SGS	3	Vis., Red	0.432	3 × 10	2.29
10	930.708	10.0	46	Fresno LX-200 406 SGS	3	Vis., Red	0.432	1 × 10	3.30
High-Resolution H α Data									
1	897.371	9.0	13	Buil Tak FS-128 LHIREs	0.07	H α	0.023	21 × 2	1.88
2	898.349	9.0	14	Buil Tak FS-128 LHIREs	0.07	H α	0.023	53 × 2	1.77
3	899.349	9.0	15	Buil Tak CN-212 HIRES	0.1	H α	0.038	31 × 2	1.78
4	901.323	9.0	17	Buil Tak CN-212 HIRES	0.1	H α	0.038	49 × 2	1.71
5	902.324	9.0	18	Buil Tak CN-212 HIRES	0.1	H α	0.038	30 × 2	1.72
6	904.330	9.0	20	Buil Tak CN-212 HIRES	0.1	H α	0.038	26 × 2	1.77

NOTE.—HJD = Heliocentric Julian Date of midexposure, Vis = visible 460–665 nm, red = 665–790 nm, H α = 648–665 nm.

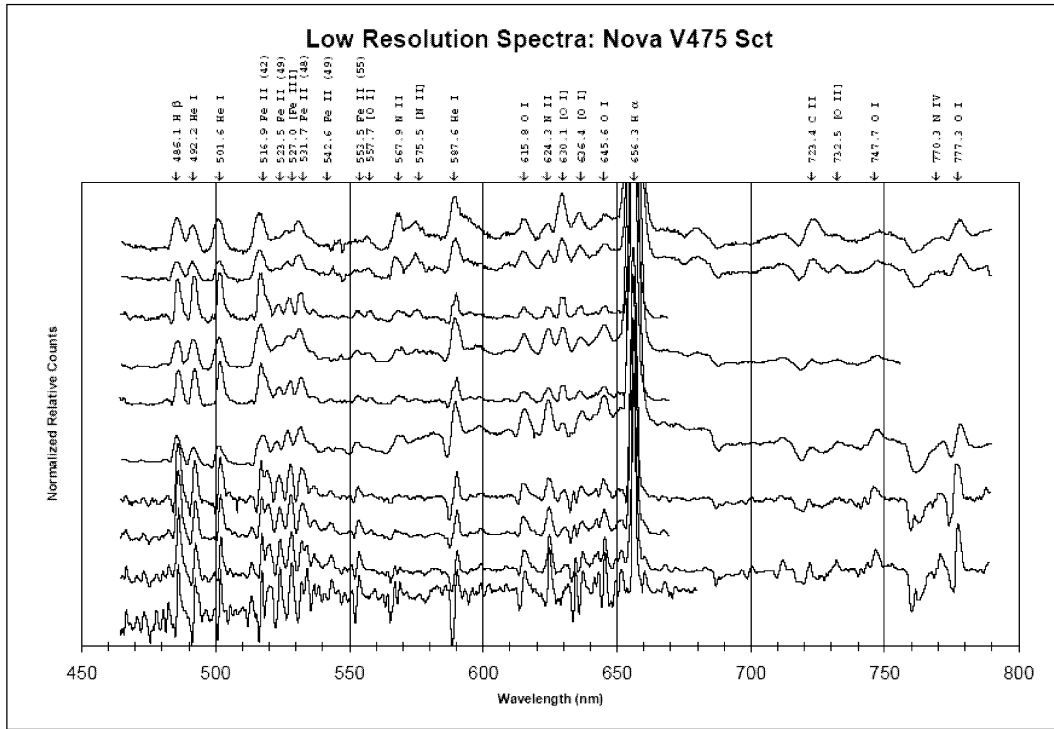


FIG. 2.—Time-staggered low-resolution spectra data, presented with the major emission lines identified. Days since maximum are noted at the left, where $T_{\max} = \text{JD } 2,452,884.3 \pm 0.5$ days. The nova displayed dominant Balmer lines and numerous Fe II multiplets (42, 48, 49, and 55) with well-distributed, strong P Cygni profiles that disappeared near the end of our observations. Spectral evolution produced low-ionization forbidden lines consistent with a Williams et al. (1994) auroral phase.

TABLE 4
MAIN SPECTRAL FEATURES AND EVOLUTION

REST WAVELENGTH (nm)	ATOMIC ID	1 DAY		2 DAYS		6 DAYS		12 DAYS		12 DAYS		24 DAYS		25 DAYS		39 DAYS		40 DAYS		46 DAYS	
		<i>v</i>	EW	<i>v</i>	EW	<i>v</i>	EW	<i>v</i>	EW	<i>v</i>	EW	<i>v</i>	EW	<i>v</i>	EW	<i>v</i>	EW	<i>v</i>	EW	<i>v</i>	EW
486.1	H β	1.3	4.5	1.3	3.7	1.5	4.3	1.3	3.6	1.6	8.3	1.8	11.7	1.8	6.9	1.9	10.6	2.0	8.1	2.0	15.4
492.4	Fe II (42)	1.3	3.5	1.3	1.6	1.3	2.2	1.3	2.4	1.4	5.3	1.7	11.0	1.8	17.4	1.7	10.1	1.9	7.5	2.1	28.3
501.8	Fe II (42)	1.1	2.3	1.1	1.5	1.3	2.7	1.2	2.0	2.0	13.2	1.8	14.7	1.8	17.4	1.7	7.9	1.7	7.1	2.1	33.6
516.9	Fe II (42)	0.7	1.4	0.9	1.2	1.2	1.8	1.0	1.4	2.4	20.3	1.7	13.1	2.3	17.6	1.8	8.7	2.3	15.5	2.3	40.7
523.5	Fe II (49)	1.2	2.7	1.2	1.0	1.6	1.6	1.4	1.0	1.3	1.2	1.6	1.7	1.6	...	1.4	1.3
527.0	[Fe III]	1.1	2.5	1.3	1.4	1.5	2.3	1.3	1.6	1.3	1.9	1.4	1.7	1.8	1.0	1.3	1.5	1.4	1.1	1.2	1.2
531.7	Fe II (48)	1.0	1.2	1.1	0.8	1.8	2.3	1.5	1.7	1.4	1.9	1.8	4.0	1.6	2.6	1.5	2.8	1.7	2.6	1.1	1.2
546.2	Fe II (49)	1.0	0.5	1.2	0.4	1.7	0.8	1.3	0.4
553.5	Fe II (55)	1.0	0.6	1.1	0.6	1.2	0.7	1.3	0.7	1.8	2.1	1.7	1.6	1.7	1.7	1.4	0.9
557.7	[O I]	1.4	0.4	1.9	0.5	1.5	1.5	1.6	1.5	1.5	1.2	1.7	3.1	1.7	8.8
567.9	N II	0.7	0.3	0.8	0.2	0.8	0.3	2.1	0.5	2.3	4.8	2.4	3.6	2.1	4.7	2.0	2.8	1.8	7.0	1.7	24.8
575.5	[N II]	1.2	0.3	1.5	0.2	1.5	0.3	1.6	0.3	3.3	1.7	2.0	4.7	2.2	3.1
587.6	He I	0.9	0.6	1.0	0.9	1.1	1.3	1.1	1.4	1.0	2.0	1.2	5.2	1.8	12.9	1.5	8.0	1.8	8.3	1.9	9.7
614.5	Fe II (74)	1.3	0.9	1.4	1.3	1.9	1.8	1.7	1.3	1.5	2.0	2.1	3.7	1.6	3.9	2.0	2.6	1.8	3.6	2.0	5.5
624.3	N II	0.8	1.3	1.3	2.1	1.3	2.1	1.5	1.6	1.4	2.6	1.7	4.3	1.6	4.2	1.6	2.1	1.5	3.2	1.5	3.5
630.1	[O I]	1.2	0.7	1.3	0.4	1.4	0.6	1.2	0.5	0.8	0.5	1.2	4.1	1.4	3.8	1.3	3.7	1.3	2.7	1.5	6.0
636.4	[O I]	1.0	0.9	0.9	0.6	1.2	0.5	1.1	0.6	1.4	1.5	1.4	1.5	1.5	2.6	1.5	1.6	1.6	2.1	1.2	2.3
645.6	Fe II (74)	0.6	0.6	0.9	1.2	1.2	1.1	1.3	1.0	1.3	1.2	1.7	2.7	1.9	3.3	1.2	0.7	1.9	1.9	1.7	2.6
656.3	H α	0.7	5.4	0.9	11.0	1.0	13.2	1.1	16.5	1.2	30.0	1.3	64.5	1.4	78.6	1.5	45.4	1.5	64.5	1.6	91.4
723.4	C II	2.4	1.0	0.9	0.5	1.3	2.5	4.3	1.8	2.2	12.4	2.7	19.0
732.5	[O II]	2.6	1.1	2.9	2.2	1.9	1.6	3.8	1.6	1.5	1.8	1.9	2.1
747.7	O I	2.8	1.1	1.3	1.1	1.5	1.7	5.4	2.2	2.7	4.5	3.1	3.9
770.8	C IV	3.1	1.2	1.8	1.8	1.8	3.4	1.9	2.1	1.6	1.3
777.3	O I	2.2	0.9	1.1	2.5	1.1	2.8	1.5	6.8	1.9	7.0

NOTE.—An atomic identification has been assigned to each of the major emission peaks. The velocity widths v are taken from the FWHM of emission line, or the emission component, when P Cygni profiles are present. The velocity widths are $\times 10^3$ km s $^{-1}$, with errors of $\leq 0.2 \times 10^3$ km s $^{-1}$. The equivalent widths (EW) are in nm, while “days” are days since maximum.

1994). The most common type of spectral transition defined by Williams et al. starts with a principal phase with extensive Fe II multiplets and without forbidden low-ionization lines. This gives way to the disappearance of the Fe II multiplets and concomitant emergence of the more common nebular forbidden lines, such as [O I], [N II], and [O III].

Figure 2 shows the spectral evolution in days (d) since maximum brightness. The spectra did follow the evolution described above. V475 Sct displayed early emission lines that included H α , H β , Fe II (multiplets of 42, 48, 49, 55, and 74), and several of He I, O I, and N II lines. Emission lines present late included many [O I], [N II], and [O II] forbidden low-ionization lines. The Fe II multiplets did not completely disappear through the end of the study at 46 days. The intensity of the emission lines only diminished by about 50%. Spectra taken after 46 days may have shown a more complete transition. The early spectra showed many peaks that exhibited strong P Cygni profiles that disappeared near the end of our observations. One of the strongest blueshifted absorption features was found to be associated with the He I 587.6 nm line. Early on, it showed an absorption velocity (FWHM) of 1200 km s $^{-1}$ and an emission velocity (FWHM) of 920 km s $^{-1}$, with the blueshifted absorption component diminishing significantly by

39 days, implying a strong outflow at the beginning of the eruption that later diminished. Table 4 shows the main spectral features and their evolution. The table includes the rest wavelength, atomic line identifications, FWHM values, velocity widths v , and equivalent widths (EW) of the major emission lines.

3.3. H α Line Profiles

Figure 3 shows the behavior of the H α line. The H α velocity width values are plotted versus time in Figure 1 on the right vertical axis. A clear trend of emission-line broadening or increasing velocity width is clear. The velocity values increased rapidly within the first few days. As the velocity continued to increase, the rate of apparent acceleration decreased. It is unclear what the driving force is behind this line broadening. It may be tied to the spectral observation of deeper, hotter and higher velocity layers of the outflow. Empirically, we observe the velocity curve to be well fitted by a natural log function:

$$v = 372.04 \times \ln t + 94.03, \quad R^2 = 0.9261,$$

where t is days following discovery.

Velocity width (v) values had corrections for instrumental

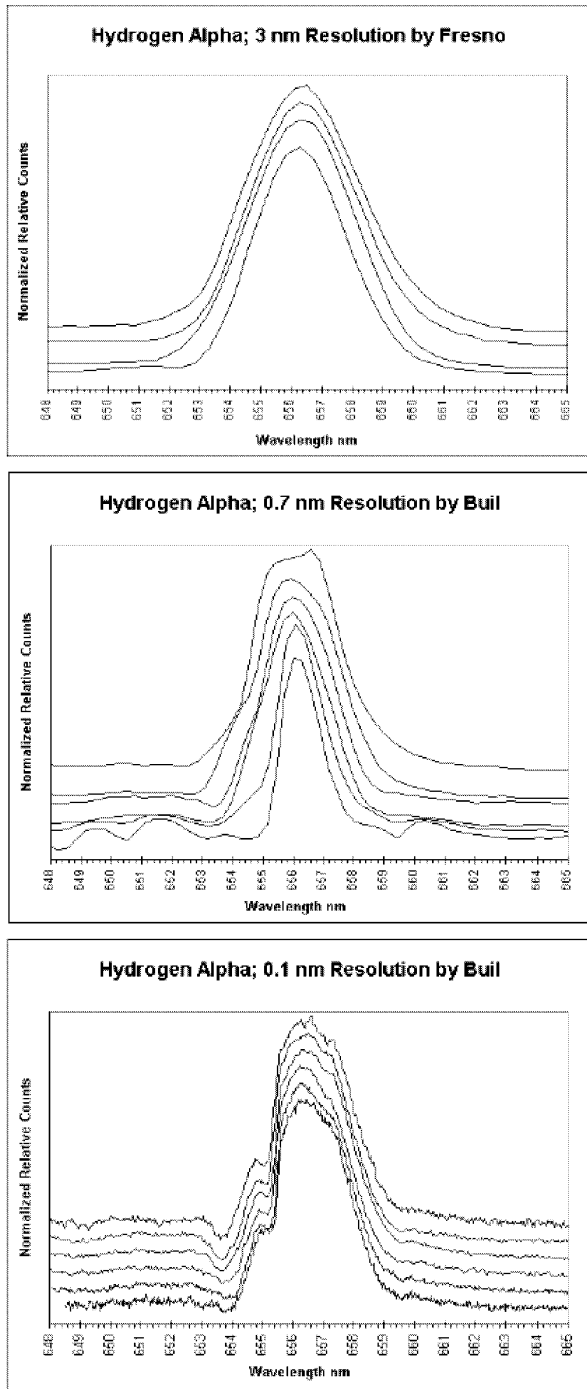


FIG. 3.—*Top*: $H\alpha$ profile with a resolution of 3 nm, Fresno setup. The four observations were made at 12, 25, 40, and 46 days after maximum, bottom to top. The velocity width increases from 1200 to $1600 \pm 200 \text{ km s}^{-1}$. *Middle*: $H\alpha$ profile with a resolution of 0.7 nm, Meris setup. The six observations were made at 1, 2, 6, 12, 24, and 39 days after maximum, bottom to top. The velocity width increases from 750 to $1500 \pm 130 \text{ km s}^{-1}$. *Bottom*: $H\alpha$ profile with a resolution of ~ 0.1 nm, HIRES setup. The six observations were made at 13, 14, 15, 17, 18, and 20 days after maximum, bottom to top. The velocity width increases from 1150 to $1275 \pm 15 \text{ km s}^{-1}$ in this short 7 day window. Note the presence of [N II] at 654.8 nm partially filling the blueshifted absorption feature.

effects, both for line broadening due to a low resolution (definitely the case for the Fresno spectra) and for adjusting the spectra to the velocity frame of the high-resolution spectra. The Meris and Fresno low-resolution optical setups produced dispersions of 0.287 and $0.432 \text{ nm pixel}^{-1}$, respectively. The instrumental-effect corrections were close to or less than a 1 pixel equivalent for the Meris and Fresno setups, at $+0.385$ and -0.405 nm , respectively.

4. CONCLUSION

The high-resolution $H\alpha$ line profiles of V475 Sct have minimal structure, unlike most novae (see, e.g., Hutchings 1972; Williams et al. 1991, 1994). This suggests that the shell had an isotropic expansion with an optically thick wind. No distinct line profile structure emerges during decline that would indicate asymmetric expansion. In this study, the $H\alpha$ emission-peak profile had minimal, if any, blueshifted absorption, unlike most of the other emission peaks analyzed early in this study. It was perhaps being partially filled by the [N II] 654.8 nm line.

The optically thick wind that was ejected from the white dwarf may be responsible for the Fe II-rich principal spectra. Our early data showed that most of the mass that was initially ejected by the nova had contributed to the development of P Cygni profiles, with their emission components oriented symmetrically about the systemic velocity. The blueshifted absorption features of the principal spectrum weakened as the nova declined from maximum brightness. By 46 days, a pure emission spectrum was observed. The spectra clearly showed that the principal spectra did not originate from a discrete shell of gas that was expelled, as in an impulse, from the white dwarf at the time of outburst.

The principal spectra made a clear transition to the auroral phase (as defined by Williams et al. 1994). Our spectra show that throughout the study, the envelope maintained an optically thick wind and was ionization-bounded (Warner 1995, p. 273). This allowed for the formation of an outer region of neutral gas and for the development of many low-ionization lines, such as [O I], [N II], and [O II]. This gave rise to the observed continued presence of Fe II lines and concurrent forbidden lines near the end of our observations.

The shape of the light curve and thus the t_2 and t_3 times depend on variations of both mass-loss and reaccretion rates. Our best estimate values for t_2 and t_3 are 22 and 52 days, respectively. V475 Sct is therefore a fast nova (Warner 1989, p. 3) with a type Ba light curve as defined by Duerbeck (1981).

Only part of the accreted material may have reached escape velocity. If this were the case, infalling matter would be reaccreted. Delayed surface burning of this backflow might account for the short plateau and minor irregular fluctuations observed in the light curve. This may explain why the $H\alpha$ profiles exhibit an optically thick, isotropic wind, and why the velocity widths were seen to double during our observations.

Many novae are observed to develop resolved nebular rem-

nants in the years following their eruptions, which are often referred to as nova shells (Cohen & Rosenthal 1983; Wade 1990). Not all novae are observed to develop nova shells, however. This may be because nova shells are faint, small, and fade within a few years, often making them difficult to observe (e.g., Slavin et al. 1995). The possibility also exists that some novae do not show nova shells because they do not have them. The slowing of the expansion velocity of the H α line in V475 Sct suggests that any expanding cloud of ejecta might eventually slow to a point at which it will not produce an optically

resolved remnant. It will therefore be interesting to monitor V475 Sct in the coming years. Will it develop a nova shell?

We thank the American Association of Variable Star Observers (AAVSO) for sending us their validated light curve of V475 Sct. We also thank the late Dr. Harold Downing, and Dr. Tom and Cynthia Downing, for donating the Downing Planetarium, on which Fresno State's Campus Observatory stands, as well as the College of Science and Mathematics, for their support.

REFERENCES

- Boeche, C., Munari, U., Liller, W., & Fujii, M. 2003, IAU Circ. 8191
 Cohen, J. G., & Rosenthal, A. J. 1983, ApJ, 268, 689
 Duerbeck, H. W. 1981, PASP, 93, 165
 Hutchings, J. B. 1972, MNRAS, 158, 177
 Morgan, G. E., Ringwald, F. A., & Prigge, J. W. 2003, MNRAS, 344, 521
 Nakano, S., Sato, H., Nishimura, H., Nakamura, T., Wakuda, S., Yamaoka, H., & Pearce, A. 2003, IAU Circ. 8190
 Samus, N., et al. 2003, IAU Circ. 8200
 Siviero, S., Marrese, P. M., Munari, U., Yamaoka, H., Monard, B., Rodriguez, D., Henden, A., & Hasubick, W. 2003, IAU Circ. 8199
 Slavin, A. J., O'Brien, T. J., & Dunlop, J. S. 1995, MNRAS, 276, 353
 Wade, R. A. 1990, in Proc. IAU Colloq. 122, Physics of Classical Novae, ed. A. Cassatella & R. Viotti (Berlin: Springer), 179
 Warner, B. 1989, in Classical Novae, ed. M. F. Bode & A. Evans (Chichester: Wiley), 3
 ———. 1995, Cataclysmic Variable Stars (Cambridge: Cambridge Univ. Press)
 Williams, R. E., Hamuy, M., Phillips, M. M., Heathcote, S. R., Wells, L., & Navarrete, M. 1991, ApJ, 376, 721 (Paper 1)
 Williams, R. E., Phillips, M. M., & Hamuy, M. 1994, ApJS, 90, 297